Atomic emission rates in inhomogeneous media with applications to photonic band structures

Jonathan P. Dowling and Charles M. Bowden
Weapons Sciences Directorate, AMSMI-RD-WS-ST, Research, Development, and Engineering Center, U.S. Army Missile Command, Redstone Arsenal, Alabama 35898-5248
(Received 29 January 1992)

There has been a great deal of interest in periodic dielectric materials that exhibit photonic band structures. One of the more interesting features of such a substance is its ability to alter the emission rate of probe atoms embedded in the periodic lattice. Large enhancements and complete inhibition of emission rates can be obtained. It has been known for some time that the influence of a cavity on atomic emission is essentially a classical effect. Hence, we develop a general classical treatment of radiation rates in an inhomogenous medium. Our results agree with those of a fully quantum calculation, and are applied to a simple scalar model of a dipole in a one-dimensional periodic lattice of the Kronig-Penney type.

PACS number(s): 42.60.Da, 03.50.De, 41.20.Bt, 42.25.Gy

I. INTRODUCTION

It was in 1946 that Purcell [1] first predicted that nontrivial boundary conditions on the electromagnetic field in the vicinity of an excited atom could alter the atomic emission rate. This hallmark effect of cavity QED has been investigated theoretically [2] and experimentally [3] in cavities with simple geometries such as conducting plane mirrors, spheres, and so forth. In the wake of the theoretical promulgation of [4] and the experimental investigation into [5], periodic dielectric lattice structures that exhibit photonic frequency passbands, and band gaps, concern has turned to the question of the behavior of atomic emission rates in such materials [6].

It has been known for some time now that the effect of a cavity on emission rates of atoms is essentially classical [7–9]. This can be seen by considering Fermi's golden rule. Suppose we have a single two-level atom coupled to the electomagnetic field. Further suppose that the atom is in an initial excited state $|i\rangle$ and the field contains no photons. The state of the system we write $|i,0_{\mathbf{k}}\rangle$, where $0_{\mathbf{k}}$ indicates the lack of photons of wave number $\mathbf{k}$. Let the final state of the system consist of the atom in some final state $|f\rangle$ after the release of a photon. The final state of the system is then $|f,1_{\mathbf{k}}\rangle$. Fermi's golden rule yields for the transition rate w_{fi} the following:

$$w_{fi}=\frac{2\pi}{\hbar}\rho(\hbar\omega_{\mathbf{k}})|\langle f,1_k|H_{\rm int}|i,0_{\mathbf{k}}\rangle|^2 , \tag{1}$$

where $H_{\rm int}$ is the interaction part of the Hamiltonian that couples the atom to the field, $\omega_{\mathbf{k}}$ is the frequency of the emitted photon, and ρ is the density of modes at that frequency with wave number $\mathbf{k}$. The contribution of a cavity is to alter the mode density ρ. But in the Wigner-Weisskopf regime the mode density is the same classically or quantum electrodynamically: whether or not you quantized those modes is of no consequence as far as the influence of the cavity is concerned. Hence, the computation of the cavity-induced emission rate can be carried out equally well classically or quantum electrodynamically, as has been shown explicitly by Morawitz and others [7–9]. In the case of photonic band materials, the existence of band gaps has been demonstrated by solving numerically the classical electromagnetic-wave eigenvalue equation [10]. Since the emission rate, as we shall demonstrate, depends only on the structure of these classical solutions, one may directly adapt these codes to the computation of atomic relaxation times without having to invoke quantum mechanics. This fact should immensely simplify such calculations since the need for working with second quantized noncommuting operators will be obviated.

In Sec. II we will develop a general classical formalism for the computation of the atomic emission rate of a point dipole inside a material with inhomogeneous dielectric constant $\epsilon(\mathbf{r})$. Our result is found to be equal to the solution found quantum electrodynamically by Glauber and Lewenstein [11]. In Sec. III we apply the formalism to the scalar case of a radiating dipole localized between a pair of perfectly reflecting, one-dimensional mirrors—a system that has several features in common with a simple one-dimensional model for a photonic band structure, discussed also in Sec. III. This latter model consists of a one-dimensional periodic array of δ-function increases in the dielectric constant—a form of the familiar Kronig-Penney model from solid-state theory [12]. We apply our formalism from Sec. II to the radiation rate of a point dipole localized inside the lattice and derive an exact formula for the emission rate. This exact analytical solution is possible due to the scalar, one-dimensional nature of the model, but it nevertheless exhibits emission quenching at photonic band-gap frequencies and also enhancement and inhibition inside the bands themselves as a function of both the dipole's location within the lattice and the dipole emission frequency.

We would like to stress that, although we apply our formalism to a scalar, one-dimensional model for ease of calculation and simplicity in interpretation, our general

theory is fully vectorial and three dimensional and is amenable to numerical methods.

II. EMISSION IN AN INHOMOGENEOUS ISOTROPIC MEDIUM

A. Derivation of the Green's function

We are interested in Maxwell's equations in a medium in which the dielectric constant $\epsilon=\epsilon(\mathbf{r})$ is position dependent, and the magnetic susceptibility $\mu=1$. These are

$$\nabla\times\mathbf{E}=-\frac{1}{c}\frac{\partial\mathbf{B}}{\partial t}\ , \tag{2a}$$

$$\nabla\times\mathbf{B}=\frac{1}{c}\epsilon(\mathbf{r})\frac{\partial\mathbf{E}}{\partial t}+\frac{4\pi}{c}\mathbf{J}\ , \tag{2b}$$

$$\nabla\cdot[\epsilon(\mathbf{r})\mathbf{E}]=4\pi\rho\ , \tag{2c}$$

$$\nabla\cdot\mathbf{B}=0, \tag{2d}$$

in Gaussian units. Since we are interested in a current source $\mathbf{J}$ that produces transverse waves that propagate, we may take the charge density $\rho\equiv0$. That implies, via the conductivity equation

$$\nabla\cdot\mathbf{J}+\frac{\partial\rho}{\partial t}=0, \tag{3}$$

that $\mathbf{J}=\mathbf{J}_\perp$ is transverse, i.e., $\nabla\cdot\mathbf{J}=0$. We may then choose a transverse gauge condition in the form

$$\nabla\cdot[\epsilon(\mathbf{r})\mathbf{A}]\equiv0 \tag{4}$$

for the vector potential $\mathbf{A}$. This gauge automatically satisfies Maxwell's equation (2c) if there is no charge. Now the absence of charge density $\rho=0$ implies that the scalar potential φ is incidentally zero. Hence, $\mathbf{E}$ and $\mathbf{B}$ are given in terms of $\mathbf{A}$ via

$$\mathbf{E}=-\frac{1}{c}\frac{\partial\mathbf{A}}{\partial t}\ , \tag{5a}$$

$$\mathbf{B}=\nabla\times\mathbf{A} \tag{5b}$$

that, when combined with Maxwell's equations (2), can be manipulated to yield the wave equation for the vector potential $\mathbf{A}$ as

$$\nabla\times\nabla\times\mathbf{A}+\frac{1}{c^2}\epsilon(\mathbf{r})\frac{\partial^2}{\partial t^2}\mathbf{A}=\frac{4\pi}{c}\mathbf{J}\ . \tag{6}$$

Let us now consider a single harmonic for the solutions of the homogeneous form of Eq. (6) with $\mathbf{J}\equiv0$. The homogeneous solutions are

$$\mathbf{A}_\mathbf{k}(\mathbf{r},t)=\mathbf{a}_\mathbf{k}(\mathbf{r})e^{-i\omega_\mathbf{k}t}\ , \tag{7}$$

where

$$\nabla\times\nabla\times\mathbf{a}_\mathbf{k}(\mathbf{r})-\frac{\omega_\mathbf{k}^2}{c^2}\epsilon(\mathbf{r})\mathbf{a}_\mathbf{k}(\mathbf{r})=0 \tag{8}$$

is the appropriate Helmholtz eigenvalue equation. We note here that it is the solution of Eq. (8), along with the dispersion relation relating $\mathbf{k}$ to $\omega_\mathbf{k}$, that is carried out—often numerically—in order to elucidate the photon band structure of the material [10]. The $\mathbf{a}_\mathbf{k}(\mathbf{r})$ obey the gauge condition

$$\nabla\cdot[\epsilon(\mathbf{r})\mathbf{a}_\mathbf{k}(\mathbf{r})]\equiv0 \tag{9}$$

and are therefore transverse with respect to this gauge. [Henceforth we shall call any vector $\mathbf{V}$ that satisfies the ϵ transverse gauge condition (9) or (4) "ϵ transverse," abbreviated "$\epsilon_\perp$."]

The $\mathbf{a}_\mathbf{k}(\mathbf{r})$ are complete in that any ϵ transverse vector may be expanded in terms of these normal modes. As Glauber and Lewenstein have pointed out [11], the appropriate completeness relation can be shown to be

$$\int d^3k\ \mathbf{a}_\mathbf{k}^*(\mathbf{r}')\mathbf{a}_\mathbf{k}(\mathbf{r})=\overleftrightarrow{\delta}_{\epsilon_\perp}(\mathbf{r}'-\mathbf{r})\ , \tag{10}$$

where $\overleftrightarrow{\delta}_{\epsilon_\perp}$ is the ϵ-transverse δ-function dyadic. This δ-function reduces to the usual free-space transverse dyadic δ function when $\epsilon(\mathbf{r})\to1$.

We are interested in how $\mathbf{A}$ propagates through an inhomogeneous medium; thus we would like to construct an $\epsilon_\perp$ propagator for $\mathbf{A}$. This we may do through the aid of the $\epsilon_\perp$ δ function and its normal-mode expansion, given in (10).

The dyadic propagator $\overleftrightarrow{\mathbf{D}}(\mathbf{r},t;\mathbf{r}',t')$ obeys the homogeneous wave equation [13]

$$\nabla_\mathbf{r}\times\nabla_\mathbf{r}\times\overleftrightarrow{\mathbf{D}}(\mathbf{r},t;\mathbf{r}',t')+\frac{1}{c^2}\epsilon(\mathbf{r})\frac{\partial^2}{\partial t^2}\overleftrightarrow{\mathbf{D}}(\mathbf{r},t;\mathbf{r}',t')=0\ , \tag{11}$$

with subsidiary conditions

$$\overleftrightarrow{\mathbf{D}}(\mathbf{r},t;\mathbf{r}',t')|_{t=t'}=0\ , \tag{12a}$$

$$\frac{\partial}{\partial t}\overleftrightarrow{\mathbf{D}}(\mathbf{r},t;\mathbf{r}',t')|_{t=t'}=c^2\overleftrightarrow{\delta}_{\epsilon_\perp}(\mathbf{r}-\mathbf{r}')\ , \tag{12b}$$

as well as meeting whatever boundary conditions are to be imposed on $\mathbf{A}$.

We distinguish between the propagator $\overleftrightarrow{\mathbf{D}}$ that satisfies the homogeneous equation (11) and the dyadic Green's function $\overleftrightarrow{\mathbf{G}}$ that satisfies the inhomogeneous wave equation

$$\nabla_\mathbf{r}\times\nabla_\mathbf{r}\times\overleftrightarrow{\mathbf{G}}(\mathbf{r},t;\mathbf{r}',t')+\frac{1}{c^2}\epsilon(\mathbf{r})\frac{\partial^2}{\partial t^2}\overleftrightarrow{\mathbf{G}}(\mathbf{r},t;\mathbf{r}',t')=\frac{4\pi}{c}\delta(t-t')\overleftrightarrow{\delta}_{\epsilon_\perp}(\mathbf{r}-\mathbf{r}')\ , \tag{13}$$

with the same equal-time conditions (12) and boundary conditions that are imposed on $\overleftrightarrow{\mathbf{D}}$. The Green's function and propagator are related via the causality condition [13]

$$\overleftrightarrow{\mathbf{G}}(\mathbf{r},t;\mathbf{r}',t')=\Theta(t-t')\overleftrightarrow{\mathbf{D}}(\mathbf{r},t;\mathbf{r}',t')\ , \tag{14}$$

where Θ is a unit Heaviside step function that turns on when $t=t'$.

The transverse propagator $\overleftrightarrow{\mathbf{D}}$, like any $\epsilon_\perp$ transverse function, may be expanded in terms of the normal modes $\mathbf{a}_\mathbf{k}(\mathbf{r})$. Using the time translation invariance, we assume an expansion of the form

$$\overleftrightarrow{\mathbf{D}}(\mathbf{r},t;\mathbf{r}',t)=\int d^3k\ \mathbf{b}_{\mathbf{k}}(\mathbf{r}')\mathbf{a}_{\mathbf{k}}(\mathbf{r})\sin[\omega_{\mathbf{k}}(t-t')]\ . \quad (15)$$

Since condition (12a) implies that $\overleftrightarrow{\mathbf{D}}$ is an odd function of $t-t'$, the sine function insures automatic satisfaction of this. The unknown coefficients $\mathbf{b}_{\mathbf{k}}$ can be determined by using condition (12b):

$$\frac{\partial}{\partial t}\overleftrightarrow{\mathbf{D}}(\mathbf{r},t;\mathbf{r}',t')|_{t=t'}=\int d^3k\ \mathbf{b}_{\mathbf{k}}(\mathbf{r}')\mathbf{a}_{\mathbf{k}}(\mathbf{r})\omega_{\mathbf{k}}$$
$$=c^2\overleftrightarrow{\delta}_{\epsilon_\perp}(\mathbf{r}'-\mathbf{r})\ . \quad (16)$$

Invoking the completeness relation (10) for the $\mathbf{a}_k$ and comparing like coefficients, we have

$$\mathbf{b}_{\mathbf{k}}(\mathbf{r}')=\frac{c^2}{\omega_{\mathbf{k}}}\mathbf{a}_{\mathbf{k}}^*(\mathbf{r}')\ , \quad (17)$$

in which case the normal-mode expansion of the propagator, the Green's function, and their time derivatives are, respectively,

$$\overleftrightarrow{\mathbf{D}}(\mathbf{r},t;\mathbf{r}',t')=c^2\int d^3k\ \mathbf{a}_{\mathbf{k}}^*(\mathbf{r}')\mathbf{a}_{\mathbf{k}}(\mathbf{r})\frac{\sin[\omega_{\mathbf{k}}(t-t')]}{\omega_{\mathbf{k}}}, \quad (18a)$$

$$\frac{\partial}{\partial t}\overleftrightarrow{\mathbf{D}}(\mathbf{r},t;\mathbf{r}',t')=c^2\int d^3k\ \mathbf{a}_{\mathbf{k}}^*(\mathbf{r}')\mathbf{a}_{\mathbf{k}}(\mathbf{r})\cos[\omega_{\mathbf{k}}(t-t')]\ , \quad (18b)$$

$$\overleftrightarrow{\mathbf{G}}(\mathbf{r},t;\mathbf{r}',t')=c^2\Theta(t-t')\int d^3k\ \mathbf{a}_{\mathbf{k}}^*(\mathbf{r}')\mathbf{a}_{\mathbf{k}}(\mathbf{r})$$
$$\times\frac{\sin[\omega_{\mathbf{k}}(t-t')]}{\omega_{\mathbf{k}}}\ , \quad (18c)$$

$$\frac{\partial}{\partial t}\overleftrightarrow{\mathbf{G}}(\mathbf{r},t;\mathbf{r}',t')=c^2\Theta(t-t')\int d^3k\ \mathbf{a}_{\mathbf{k}}^*(\mathbf{r}')\mathbf{a}_{\mathbf{k}}(\mathbf{r})$$
$$\times\cos[\omega_{\mathbf{k}}(t-t')]\ . \quad (18d)$$

We see that the Green's function obeys the wave equation and the correct boundary conditions since the $\mathbf{a}_{\mathbf{k}}$ do.

B. The power output of a localized source in the medium

We are interested in how the inhomogeneous medium affects the emission rate of a localized source. The idea is as follows: A current density $\mathbf{J}$ that is radiating will be immersed in its own electric field that has been emitted at earlier times and that has been reflected from inhomogeneities in the medium. The Green's function may be used to address the problem of determining this field since $\overleftrightarrow{\mathbf{G}}$ contains all information about $\epsilon(\mathbf{r})$ and boundary conditions through its dependence on the normal-mode eigenfunctions $\mathbf{a}_{\mathbf{k}}(\mathbf{r})$. The rate at which a current density source $\mathbf{J}$ does work against a surrounding electric field $\mathbf{E}$ is given by [14]

$$P(t)=-\int_V dV\,\mathbf{J}(\mathbf{r},t)\cdot\mathbf{E}(\mathbf{r},t)\ , \quad (19)$$

where V is a volume containing $\mathbf{J}$. From Eq. (5a), relating $\mathbf{E}=-(1/c)\partial\mathbf{A}/\partial t$, we can write

$$P(t)=\frac{1}{c}\int_V dV\,\mathbf{J}(\mathbf{r},t)\cdot\frac{\partial\mathbf{A}(\mathbf{r},t)}{\partial t}\ . \quad (20)$$

Now in the absence of any externally applied fields, the inhomogeneous wave equation, Eq. (6), can be formally solved for $\mathbf{A}$ in terms of $\mathbf{J}$ via the Green's function $\overleftrightarrow{\mathbf{G}}$ as

$$\mathbf{A}(\mathbf{r},t)=\frac{4\pi}{c}\int_{-\infty}^{\infty}dt'\int_V dV'\overleftrightarrow{\mathbf{G}}(\mathbf{r},t;\mathbf{r}',t')\cdot\mathbf{J}(\mathbf{r}',t)$$
$$=\frac{4\pi}{c}\int_{-\infty}^{t}dt'\int_V dV'\overleftrightarrow{\mathbf{D}}(\mathbf{r},t;\mathbf{r}',t')\cdot\mathbf{J}(\mathbf{r}',t')\ , \quad (21)$$

where we have used Eq. (14) relating $\overleftrightarrow{\mathbf{G}}$ and $\overleftrightarrow{\mathbf{D}}$.

Combining Eq. (19) for the power output with the solution, Eq. (21), for $\mathbf{A}$, we have

$$P(t)=\frac{2\pi}{c^2}\int_{-\infty}^{t}dt'\int_V dV\int_V dV'\,\mathbf{J}(\mathbf{r},t)\cdot\left[\frac{\partial}{\partial t}\overleftrightarrow{\mathbf{D}}(\mathbf{r},t;\mathbf{r}',t')\right]\cdot\mathbf{J}(\mathbf{r}',t')$$
$$=2\pi\int d^3k\int_{-\infty}^{t}dt'\int_V dV\int_V dV'[\mathbf{J}(\mathbf{r},t)\cdot\mathbf{a}_{\mathbf{k}}(\mathbf{r})][\mathbf{J}(\mathbf{r}',t')\cdot\mathbf{a}_{\mathbf{k}}^*(\mathbf{r}')]\cos[\omega_{\mathbf{k}}(t-t')]\ , \quad (22)$$

where we have used the modal expansion (18b) for $\partial\overleftrightarrow{\mathbf{D}}/\partial t$ and we also have used the fact that $\overleftrightarrow{\mathbf{D}}$ is an odd function of $t-t'$. The Leibnitz formula was used to carry the $\partial/\partial t$ operator past the integral $\int_{-\infty}^{t}dt'$.

We now derive a remarkably simple formula for the total energy $U(T)=\int_{-\infty}^{T}dt\,P(t)$ that has been emitted by our localized source up to time T:

$$U(T)\equiv\int_{-\infty}^{T}dt\,P(t)$$
$$=2\pi\int d^3k\int_{-\infty}^{T}dt\int_{-\infty}^{t}dt'\int_V dV\int_V dV'[\mathbf{J}(\mathbf{r},t)\cdot\mathbf{a}_{\mathbf{k}}(\mathbf{r})][\mathbf{J}(\mathbf{r}',t')\cdot\mathbf{a}_{\mathbf{k}}^*(\mathbf{r}')]\cos[\omega_{\mathbf{k}}(t-t')]$$
$$=\pi\int d^3k\left|\int_{-\infty}^{T}dt\int_V dV\,\mathbf{J}(\mathbf{r},t)\cdot\mathbf{a}_{\mathbf{k}}(\mathbf{r})e^{-i\omega_{\mathbf{k}}t}\right|^2\ , \quad (23)$$

where we have used

$$\cos[\omega_{\mathbf{k}}(t-t')]=\mathrm{Re}\{\exp[i\omega_{\mathbf{k}}(t-t')]\}$$

and the integration change of variables

$$\int_{-\infty}^{T}dt\int_{-\infty}^{t}dt'\rightarrow\tfrac{1}{2}\int_{-\infty}^{T}dt\int_{-\infty}^{T}dt'$$

to arrive at the separated form in the last line of Eq. (23). (See Ref. [13]). This is one of our primary results. This

formula shows exactly how energy accumulates over time in the field as a function of variations in the boundary conditions and also the medium—information that is contained in the normal-mode solutions $\mathbf{a}_{\mathbf{k}}(\mathbf{r})$.

We are primarily interested in embedding a radiating probe in, say, a photonic band material with periodically varying $\epsilon(\mathbf{r})$ and then seeing how the radiation rate responds to the surrounding medium. The simplest current density $\mathbf{J}$ would be for an oscillating point dipole. Hence we take

$$\mathbf{J}(\mathbf{r},t)=\omega_0\boldsymbol{\mu}\cos(\omega_0 t)\Theta(t)\delta(\mathbf{r}-\mathbf{r}_0) \tag{24}$$

for a harmonically oscillating point dipole with frequency ω_0 located at $\mathbf{r}_0$ with real dipole moment $\boldsymbol{\mu}$ that is turned on by the Θ function at $t=0$. Inserting this current density into Eq. (23) for the energy $U(t)$, we can carry out the time integration to obtain

$$U(t)=\pi\omega_0^2\mu^2\int d^3k\,|\mathbf{a}_{\mathbf{k}}(\mathbf{r}_0)\cdot\hat{\boldsymbol{\mu}}|^2\frac{\sin^2[(\omega_0-\omega_{\mathbf{k}})t/2]}{(\omega_0-\omega_{\mathbf{k}})^2}, \tag{25}$$

where we have dropped a "counterrotating" term containing $e^{-i(\omega_0+\omega_{\mathbf{k}})t}$ that will yield no contribution to the $\mathbf{k}$ integration in the limit $t\to\infty$. We can now compute the steady-state rate of power emission by considering $P(t)=U'(t)$ in the limit $t\to\infty$ when all transients arising from the sharp turn-on at $t=0$ have died away:

$$\begin{aligned}P(t)&=U'(t)\\&=\pi^2\omega_0^2\mu^2\int d^3k\,|\mathbf{a}_{\mathbf{k}}(\mathbf{r}_0)\cdot\hat{\boldsymbol{\mu}}|^2\frac{\sin[2(\omega_0-\omega_{\mathbf{k}})t]}{2\pi(\omega_0-\omega_{\mathbf{k}})}\\&\underset{t\to\infty}{\to}\frac{\pi^2}{2}\omega_0^2\mu^2\int d^3k\,|\mathbf{a}_{\mathbf{k}}(\mathbf{r}_0)\cdot\hat{\boldsymbol{\mu}}|^2\delta(\omega_0-\omega_{\mathbf{k}})\\&\equiv P(\infty)\,,\end{aligned} \tag{26}$$

where we have used a standard representation of the δ function,

$$\lim_{a\to\infty}\frac{\sin(ax)}{\pi x}=\delta(x)$$

and the fact that $\delta(bx)=\delta(x)/|b|$; also, $\hat{\boldsymbol{\mu}}\equiv\boldsymbol{\mu}/|\boldsymbol{\mu}|$. We may not in general simplify this further since $\mathbf{k}$ depends on $\omega_{\mathbf{k}}$ in a nontrivial way through the dispersion relation. It is interesting, however, to note that the power output of a point dipole is localized in space and in frequency. Only those modes that satisfy the condition $\omega_{\mathbf{k}}=\omega_0$ affect the emission rate, and they do so only at the location of the dipole at $\mathbf{r}=\mathbf{r}_0$. As we mentioned earlier, we see now that the effect of the medium on emission rates is a classical phenomenon. It is comforting then that our classically derived formula (26) for the power output agrees with the fully quantum electrodynamical result for spontaneous emission rates of a two-level atom obtained by Glauber and Lewenstein [11]. Hence, to compute the effect of an inhomogeneous medium on a dipole emission rate, one may use our formula with classically generated normal-mode functions $\mathbf{a}_{\mathbf{k}}$, solutions of the Helmholtz equation (8), without fear that some quantum feature is being overlooked. The formula (25) then lends itself for numerical calculation with the present computer codes that generate $\mathbf{a}_{\mathbf{k}}(\mathbf{r})$ classically for various different photonic band structures.

As a simple exercise in using the power formula, Eq. (26), we apply it to the computation of the steady-state power radiated by a point dipole in free space. The appropriate normal modes are

$$\mathbf{a}_{\mathbf{k}}(\mathbf{r})=(2\pi)^{-3/2}e^{-i\mathbf{k}\cdot\mathbf{r}}\hat{\mathbf{e}}_{\mathbf{k}}\,, \tag{27}$$

where the dielectric constant $\epsilon(\mathbf{r})=1$, and $\hat{\mathbf{e}}_{\mathbf{k}}$ is a polarization vector with $\hat{\mathbf{e}}_{\mathbf{k}}\cdot\mathbf{k}=0$ for our transverse waves. Inserting this into Eq. (26) for the power output, we obtain

$$\begin{aligned}P^{\text{free 3D}}_{(-\infty)}&=\frac{1}{16\pi}\frac{\omega_0^4\mu^2}{c^3}\int d\Omega_{\mathbf{k}}|\hat{\mathbf{e}}_{\mathbf{k}}\cdot\hat{\boldsymbol{\mu}}|^2\\&=\frac{\omega_0^4\mu^2}{c^3}\int d\Omega_{\mathbf{k}}\sin^2\theta_{\mathbf{k}}=\frac{1}{2}\left[\frac{1}{3}\frac{\omega_0^4\mu^2}{c^3}\right]\end{aligned} \tag{28}$$

which, when multiplied by a factor of 2 to account for the two possible polarization degrees of freedom, yields the usual free-space result for the time-averaged power [14].

In Sec. III we find the normal modes $\mathbf{a}_{\mathbf{k}}(\mathbf{r})$ for a simple one-dimensional, scalar model for a photonic band structure. Using these, we may track the radiation rate of a one-dimensional point dipole probe in such a material.

III. EMISSION RATES IN A PHOTONIC BAND STRUCTURE

We now turn to an investigation of atomic emission rates in two simple, one-dimensional systems. First we consider a point dipole radiating between a pair of perfectly conducting, one-dimensional mirrors. This exercise illustrates several features that appear when we treat the case of a dipole radiating in a photonic band structure described by a one-dimensional Kronig-Penney model.

A. Emission between parallel mirrors in one dimension

We consider a simple one-dimensional model such that only modes $\mathbf{a}_{\mathbf{k}}$ where $\hat{\mathbf{e}}_{\mathbf{k}}\cdot\hat{\boldsymbol{\mu}}=1$ are considered, where $\hat{\boldsymbol{\mu}}=\boldsymbol{\mu}/|\boldsymbol{\mu}|$; i.e., only modes polarized parallel to the dipole moment in one dimension are included. We imagine these modes to be confined by parallel one-dimensional mirrors with a radiating point dipole $\boldsymbol{\mu}$ located between the mirrors as shown in Fig. 1. The normal modes in this case are

$$\mathbf{a}_{\mathbf{k}}(\mathbf{r})=a_{k_n}(x)=\left[\frac{2}{d}\right]^{1/2}\sin(k_n x)\,, \tag{29}$$

where the discrete set of wave numbers k_n are given by

$$k_n=\frac{\omega_n}{c}=\frac{n\pi}{d},\quad n=1,2,3,\ldots \tag{30}$$

and where d is the mirror spacing. Physically, the only allowable modes are those such that an integral number of half-wavelengths $\lambda_n/2=d/n$ fit between the mirrors.

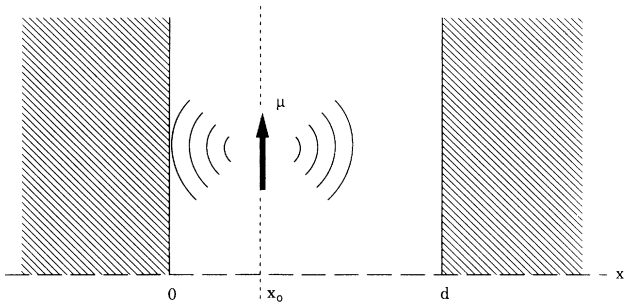

FIG. 1. Here we show an oscillating point dipole of dipole moment μ and frequency ω_0 located at a point $x_0 \in (0,d)$ between a pair of one-dimensional, perfectly conducting mirrors of separation d. Only electromagnetic radiation that is resonant with the cavity at one of the discrete frequencies $\omega_n = k_n c = 2\pi c/\lambda_n$ will be allowed, where an integral number of half-wavelengths fit between the mirrors, i.e., $n(\lambda_n/2) = d$ for $n = 1,2,3,\ldots$. This simple model has elements of photonic band structure. Infinitely narrow "bands" occur for cavity-resonant frequencies $\omega = \omega_n$, and photonic "band gaps" correspond to the nonresonant frequencies $\omega \neq \omega_n$. The dipole will radiate only if its oscillation frequency $\omega_0 = \omega_n$, i.e., when the dipole frequency lies in a band. Inside the band the dipole radiates according to Eq. (36) which is plotted in Fig. 2.

The discrete-mode, one-dimensional analog for the power-output formula (26) can be written

$$P^{\text{disc 1D}}(\infty) = \frac{\pi^2}{2}\frac{\omega_0^3 \mu^2}{c^2}\sum_n |a_{k_n}(x_0)|^2 \delta_{nn_0} , \tag{31}$$

where the Kroniker δ function contributes only if the dipole oscillation frequency $\omega_0 = n_0 \pi c/d$ is one of the discrete resonant frequencies ω_n. Inserting the mirror normal-mode functions (29) into this power expression (31), we obtain

$$P^{\text{mirr 1D}}(\infty) = \pi^2 \frac{\omega_0^2 \mu^2}{dc^2}\sum_{n=1}^{\infty} |\sin K_n x_0|^2 \delta_{nn_0} , \tag{32}$$

where $K_n \equiv \omega_n/c$.

In order to normalize this in a convenient fashion, we calculate the one-dimensional "free-space" power given by the continuum-mode expression

$$P^{\text{cont 1D}}(\infty) = \frac{\pi^2}{2}\frac{\omega_0^4 \mu^2}{c^2}\int dk\, |a_k(x_0)|^2 \delta(\omega_0 - \omega_k) , \tag{33}$$

with the one-dimensional plane wave modes

$$a_k(x_0) = \left[\frac{1}{2\pi}\right]^{1/2} e^{-ikx} , \tag{34}$$

which, when inserted into (33), yields

$$P^{\text{free 1D}}(\infty) = \frac{\pi}{4}\frac{\omega_0^4 \mu^2}{c^3} . \tag{35}$$

We now normalize the output between mirrors, Eq. (32), to the free-space output, Eq. (35), to obtain the unitless power $p(\alpha,\xi)$ as

$$\begin{aligned} p^{\text{mirr 1D}}(\alpha,\xi) &= \frac{P^{\text{mirr 1D}}(\infty)}{P^{\text{free 1D}}(\infty)} \\ &= \pi \frac{c}{\omega d}\sum_n \sin^2(K_n x)\delta_{nn'} \\ &= \pi \sum_n \frac{\sin^2 \alpha_n \xi}{\alpha_n}\delta_{nn'} , \end{aligned} \tag{36}$$

where we have defined the unitless parameters $\alpha = Kd = \omega d/c$,

$$\alpha_n \equiv \omega_n d/c = n\pi, \quad n = 1,2,3,\ldots$$

and

$$\xi \equiv x/d .$$

We have also dropped the subscripts naught on the dipole frequency $\omega_0 \to \omega$ and position $x_0 \to x$. Again, only resonant frequencies $\omega = \omega_n' = n'\pi c/d$ are selected by the

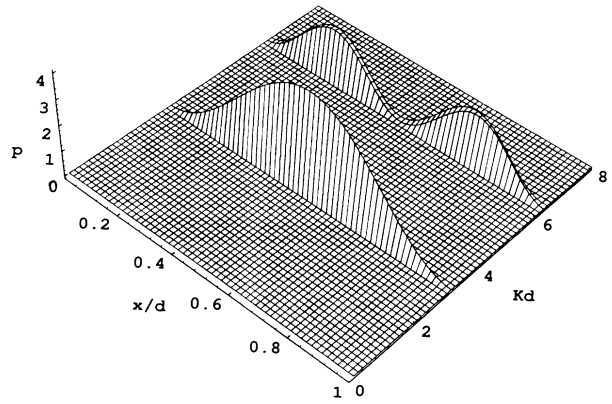

FIG. 2. Here we plot the free-space-normalized power output for a point dipole between mirrors (Fig. 1), namely, $p = p(Kd, x/d)$ from Eq. (36). Here $K = \omega/c$, where ω is the dipole oscillation frequency, and $x \in (0,d)$ is the dipole location, where d is the mirror separation, as shown in Fig. 1. The power p has been normalized such that the plane $p = 1$ corresponds to the one-dimensional free-space rate, Eq. (35). We see that the dipole radiates only when tuned to the resonant photonic "band" frequencies, $\omega = \omega_n$, $(Kd = n\pi)$ which occur when an integral number of half-wavelengths fit between the mirrors. Frequencies $\omega \neq \omega_n$ correspond to 'band gaps" in which the dipole does not radiate. Inside the bands the radiation rate is controlled by the norm square of the normal-mode wave function $a_{\omega/c}(x)$ given by Eq. (29). The radiation rate is always proportional to $|a_{\omega/c}(x)|^2$, a feature of the general theory [see Eq. (26)]. Hence, the minima and maxima of the power p rise and fall in the x direction with functional dependence $\sin^2(k_n x)$ of the normal modes, Eq. (29). Quantum electrodynamically, $|a_{\omega/c}(x)|^2$ gives the intensity of the vacuum field between the mirrors which drives the spontaneous emission rate of an actual atom. Hence, in classical theory (or QED) the dipole (or two-level atom) radiates maximally at the antinodes and minimally at the nodes of the normal-mode function $|a_{\omega/c}(x)|^2$—whether or not this mode is quantized.

δ function, and hence only when the dipole is tuned to these frequencies will it radiate. (The index n varies discretely with changing dipole frequency, and n' indicates a resonance of the cavity.) We plot this function $p(\alpha,\xi)$ as a function of the unitless frequency and position parameters, α and ξ, respectively, in Fig. 2. We see that there are infinitely narrow "bands" of dipole frequencies $\omega=\omega_{n'}$ where the dipole will radiate. Outside these bands, the cavity sustains no normal modes of the correct frequency—these are the "band gaps"—and the dipole does not radiate. So already we can visualize even a simple one-dimensional system consisting of a parallel mirror cavity, in some sense, as a photonic band structure. In the dipole position variable ξ, we see what is evident from the general power formula (26), namely, that the radiation rate is proportional to the norm-squared normal-mode wave function whose frequency corresponds to that of the dipole, i.e., $p \propto |a_{\omega/c}(x)|^2$. Radiation rates are hence maximal at the modal antinodes and minimal at the nodes. This is a general feature of atomic emission rates in any medium and is suggestive of what we would expect quantum electrodynamically where the $\mathbf{a}_{\mathbf{k}}(\mathbf{r})$ are quantized vacuum modes that drive the spontaneous emission rate. In Sec. III B we consider a one-dimensional Kronig-Penney model and compare and contrast the results to those found here for the pair of one-dimensional mirrors.

B. Emission rate in a one-dimensional photonic band structure

We consider a one-dimensional medium in which there are periodic δ-function increases in the dielectric "constant" of period d, as illustrated in Fig. 3. We write the dielectric constant as

$$\epsilon(x)\equiv\epsilon_0+gd\sum_{n=-\infty}^{\infty}\delta(x-nd)\ , \tag{37}$$

where g is a unitless constant that measures the δ-function strength. This model is also applicable to a three-dimensional, scalar, photonic band structure proposed by John and Wang [15]. We now must use Eq. (37) for $\epsilon(x)$ to find the one-dimensional normal modes $a_k(x)$ for this periodic structure. In one dimension the Helmholtz equation (8) for $\mathbf{a}_{\mathbf{k}}(\mathbf{r})$ reduces to

$$a''(x)+\frac{\omega_k^2}{c^2}\epsilon(x)a(x)=0\ . \tag{38}$$

Continuity of the electric field requires that

$$a(nd+0^+)-a(nd+0^-)=0,\quad n=0,\pm1,\pm2,\ldots\ . \tag{39a}$$

Due to the δ singularity, the usual requirement of continuity of the magnetic field, or, equivalently, the continuity of $a'(x)$ does not hold. However, the correct condition can be written in terms of $a'(x)$ by integrating the Helmholtz equation (38) directly over a small region $|x-nd|\leq\epsilon$ at the location nd of each δ function to obtain the second boundary condition [12], namely,

$$a'(nd+0^+)-a'(nd+0^-)+gdK^2a(nd+0)=0\ , \tag{39b}$$

where $K\equiv\omega/c$. [An alternative derivation of these boundary conditions, Eq. (39), is given in the Appendix.]

Let us consider in Fig. 3 the two regions $\mathrm{I}\equiv(0,d)$ and $\mathrm{II}\equiv(-d,0)$. In region I we make the sensible *ansatz* that $a_k(x)$ is a superposition of left- and right-going waves of frequency $\omega\equiv Kc$, a reasonable assumption, since

$$a_{\mathrm{I}}''(x)+K^2a_{\mathrm{I}}(x)=0,\quad 0<x<d \tag{40a}$$

and

$$a_{\mathrm{II}}''(x)+K^2a_{\mathrm{II}}(x)=0,\quad -d<x<0\ . \tag{40b}$$

Hence, we write

$$a_{\mathrm{I}}(x)=Ae^{iKx}+Be^{-iKx}\ . \tag{41a}$$

For convenience, from here on we have taken $\epsilon_0=1$, Eq. (37). Now in region II we will also have a superposition of left- and right-going waves, but the solution here must be related to that in I by Bloch's theorem, as a result of the periodicity of the lattice. Hence [12],

$$a_{\mathrm{II}}(x)=e^{-ikd}(Ae^{iK(x+d)}+Be^{-iK(x+d)}), \tag{41b}$$

where k is the wave number of the overall solution $a_k(x)$, still to be found. By demanding that a_{I} and a_{II} obey the boundary conditions, Eq. (39), at $x=0$, we obtain the following matrix equation for the unknown coefficients A and B:

$$\hat{M}\begin{bmatrix}A\\B\end{bmatrix}=\begin{bmatrix}0\\0\end{bmatrix}, \tag{42}$$

where

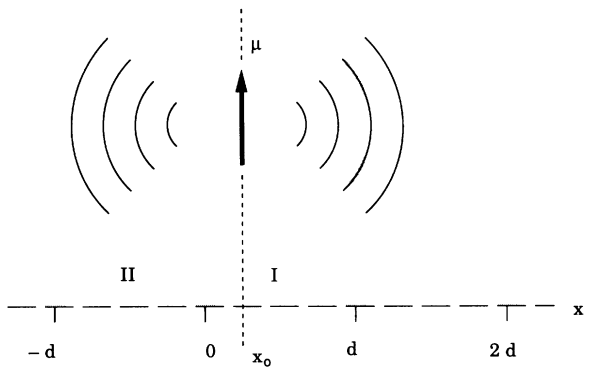

FIG. 3. Here we show a one-dimensional Kronig-Penney model for a photonic band structure that consists of an array of δ-function increases in the dielectric constant $\epsilon(x)$, Eq. (37). We locate a point dipole of frequency ω_0 at a position $x_0\in(0,d)\equiv\mathrm{I}$ in the first period of the lattice. (From periodicity, the radiation rate in other periods will be the same.) The normal-mode wave functions $a_k(x)$, Eq. (41a), in the lattice period region I are derived by applying Blochs' theorem and appropriate boundary conditions at the δ functions, in particular between regions I and II.

$$\hat{M}=\begin{bmatrix} 1-e^{-i\gamma^-} & 1-e^{-i\gamma^+} \\ 1-e^{-i\gamma^-}-ig\alpha & -1+e^{-i\gamma^+}-ig\alpha \end{bmatrix} . \quad (43)$$

Here, we have defined the following unitless parameters: $\alpha\equiv Kd\equiv\omega d/c$, $\beta=kd$, $\gamma^{\pm}\equiv\beta\pm\alpha$. The homogeneous algebraic equation (42) has a nontrivial solution if and only if the determinant $\det|\hat{M}|=0$. In this case there are an infinite number of solutions corresponding to the one-dimensional kernel of the transformation matrix $\hat{M}$. The condition $\det|\hat{M}|\equiv 0$ reduces to the dispersion relation

$$\cos\beta=\cos\alpha-\frac{g}{2}\alpha\sin\alpha\equiv f_g(\alpha) , \quad (44)$$

which relates the wave number k to the frequency ω from $\beta=kd$ and $\alpha=\omega d/c$. We plot the right-hand side of Eq. (44), defined to be the function $f_g(\alpha)$, in Fig. 4 for $g=2$. Since the cosine function always has a range $|\cos\beta|\le 1$, we see that Eq. (44) has a solution only if $|f_g(\alpha)|\le 1$. We plot the step functions $\pm\Theta(1-|f_g(\alpha)|)$ also in Fig. 4 as solid dark lines and we see that the passbands are the regions enclosed by solid rectangles. The functions ± 1 are plotted as dashed lines and show up at the band gaps that appear when $|f_g(\alpha|)>1$. We have found that the requirement for the existence of a solution of the matrix equation (42) is the satisfaction of the dispersion relation (44). When the dispersion relation is not satisfied, we are in a band gap, and Eq. (44) has only the trivial solution $A\equiv B\equiv 0$; therefore, we have no normal-mode solution. Hence, since from Eq. (26) the atomic radiation rate is proportional to $|a_k(x)|^2$ at the frequency of the dipole, we can see that at frequencies in the band gap the probe dipole cannot radiate. To see this explicitly, let us continue to solving Eq. (42) explicitly for the coefficients A and B. Recalling that $\det|\hat{M}|\equiv 0$ implies an infinite number of solutions (the kernel of the matrix transformation has dimension 1), we are free to choose *one* of A or B to be any nonzero constant. We may constrain this choice by imposing the overall normalization of the wave function as

$$\int dx\, a_{k'}^*(x)a_k(x)=\delta(k'-k) .$$

Such a choice yields

$$A=\frac{(1-e^{-i\gamma^+})}{[8\pi(\sin^2\gamma^+/2+\sin^2\gamma^-/2)]^{1/2}} , \quad (45a)$$

$$B=-\frac{(1-e^{-i\gamma^-})}{[8\pi(\sin^2\gamma^+/2+\sin^2\gamma^-/2)]^{1/2}} , \quad (45b)$$

where $\gamma^{\pm}\equiv\beta\pm\alpha$, in which case $a_{\rm I}$ and $a_{\rm II}$ are solutions in regions I and II, Fig. 3, given by Eq. (41).

Without loss of generality, we focus on the power output of a point dipole localized in region I and then note that our result may be extended to all of $x\in(-\infty,\infty)$ by periodicity.

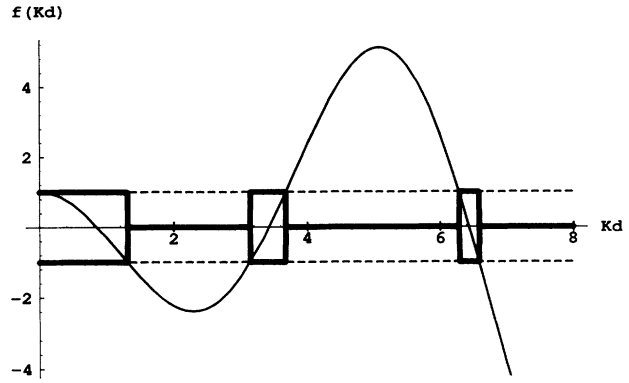

FIG. 4. Conditions for the existence of a normal-mode solution $a_k(x)$ in the lattice of Fig. 3 imply a dispersion relation relating the overall wave number k with the modal frequency ω, Eq. (44). The right-hand side of this relation, $f_g(Kd)$, is plotted here as a function of $Kd=\omega d/c$. The dark solid rectangles are generated by the step functions $\Theta(1-|f_g(Kd)|)$ and enclose the photonic band frequencies. We also plot as dashed lines $f=\pm 1$ which demonstrate band gaps when the curve f_g obeys $|f_g(Kd)|>1$.

Taking Eq. (33) for the one-dimensional power output, using $\xi=x/d$, $\xi_0=x_0/d$, and $\alpha=Kd=\omega d/c$, and $\alpha_0=K_{0\alpha}d=\omega_0 d/c$, we can write

$$P=\frac{\pi^2}{2}\frac{\omega_0^4\mu^2}{c^3}\int d\beta|a_\beta(\xi_0)|^2\delta(\alpha_0-\alpha), \quad (46)$$

where $\alpha=\alpha(\beta)$ via the dispersion relation (44). Since the integration is with respect to β but the δ function acts on $\alpha=\alpha(\beta)$, we find it convenient to change variables by implicitly differentiating the dispersion relation (44) to obtain the mode density expression

$$d\beta=\left[\sin\alpha+\frac{g}{2}(\sin\alpha+\alpha\cos\alpha)\right]\frac{d\alpha}{\sin\beta_\alpha} , \quad (47)$$

where we now view $\beta=\beta(\alpha)$. We now may construct $|\alpha_\beta(\xi_0)|^2$ from Eq. (41a) for $a_{\rm I}(x)$ using the definitions (45) for the coefficients A and B. This is put into the power formula (46) and the integration carried out using the change of variable, Eq. (47). If we now divide by the one-dimensional free-space power, Eq. (35), we obtain the normalized power output in the photonic band structure as

$$p(\alpha,\xi)=\left[1-\frac{1}{2}\frac{\cos2\alpha\xi-2\cos\beta\cos[2\alpha(\xi-\frac{1}{2})]+\cos[2\alpha(\xi-1)]}{\sin^2[(\beta+\alpha)/2]+\sin^2[(\beta-\alpha)/2)]}\right]\frac{\sin\alpha+\frac{g}{2}(\sin\alpha+\alpha\cos\alpha)}{\sin\beta}\Theta(1-|f_g(\alpha)|) , \quad (48)$$

where $\beta=kd$ is taken as a function of $\alpha=\omega d/c$ from the dispersion relation, Eq. (44), as

$$\beta=\beta(\alpha)=\arccos[f_g(\alpha)] =\arccos\left[\cos\alpha-\frac{g}{2}\alpha\sin\alpha\right] . \quad (49)$$

We have dropped the subscripts on the dipole parameters $\alpha_0\to\alpha$ ($\omega_0\to\omega$) and $\xi_0\to\xi$ ($x_0\to x$) since no other values of frequency and position now appear. The step function $\Theta(1-|f_g(\alpha)|)$ explicitly ensures the enforcement of zero power output in the band gaps, as noted earlier. We plot the power as a two-dimensional surface in Fig. 5 as a function of $\alpha=Kd=\omega d/c$, the dipole frequency parameter, and $\xi=x/d\in(0,1)$, the dipole location parameter in region I of Fig. 3. In Fig. 5(a) we restrict the range of

$$\alpha=Kd\in(0,4)\cong(0,0.127\pi)$$

in order to show the details of the bands that begin at $\alpha=0$ and π. [From the dispersion relation, Eq. (44), we see that the bands always begin at $\alpha=Kd=n\pi$, $n=0,1,2,\ldots$] The zeroth-order band is in the approximate range $\alpha\in(0,0.42\pi)$, as can be seen also in the plot of the dispersion relation, Fig. 4. The dipole radiates close to the free-space value, the plane $p=1$, until α reaches the trailing edge of the zeroth-order band. At the band edge the mode density increases somewhat—a phenomenon known from solid-state theory—and so the dipole radiation rate [which is proportional to the mode density by the classical analog of Fermi's golden rule, Eq. (1)] increases also. The power shuts off as we enter the band gap only to turn on at $\alpha=\pi$ when we enter the first-order band that extends in frequency from $\alpha=\pi$ to about $\alpha=1.17\pi$. Once again, we see an atomic emission rate increase near the trailing band edge. In order to understand the behavior of $p(\alpha,\xi)$ as a function of $\xi=x/d$, we consider Fig. 5(b) where we extend the range of α to $\alpha=8\cong2.55\pi$ in order to include the narrow second-order band beginning at $\alpha=2\pi$ and ending at 2.10π. We notice the strong similarities between Fig. 5(b) and Fig. 2 for the radiation rate of a dipole between a pair of parallel mirrors of separation d. Notice that between mirrors the "bands" of measure zero are located at $\alpha=Kd=n\pi$, while this condition implies only the *beginning* of a true band in the photonic band material. Bands occur in the mirrors at the resonance frequencies $\omega_n=2\pi c/\lambda_n$, when $\lambda_n/2=n/d$, or an even number of half-wavelengths fit between the mirrors of spacing d. In comparison, in the photonic band material the bands *begin* when $\omega_n=2\pi c/\lambda_n$, where an even number of half-wavelengths fit between each pair of δ functions of spacing d. As in

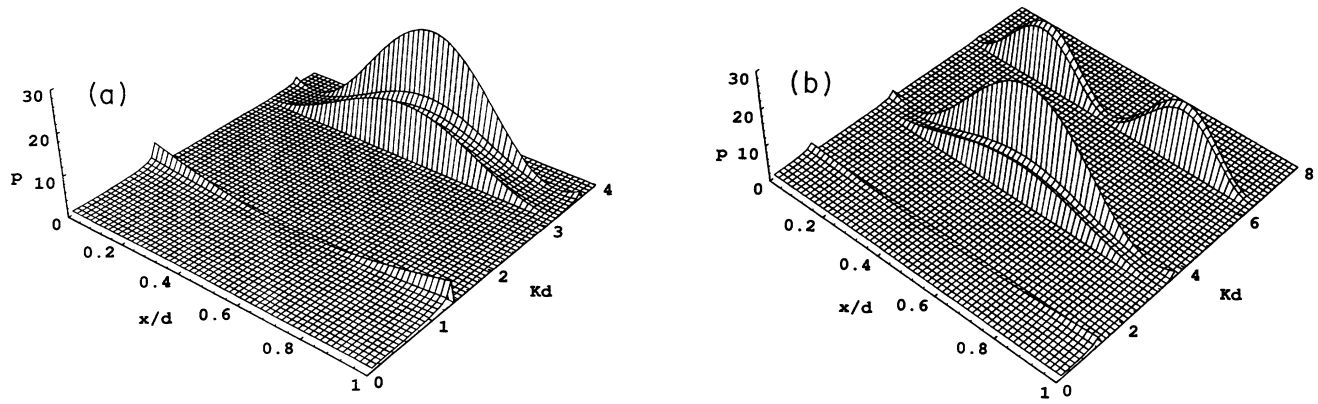

FIG. 5. Here we plot the dipole power output $p=p(Kd,x/d)$ as a function of the dipole frequency $\omega=Kc$ and dipole position $x\in(0,d)$ in region I, Fig. 3. Again, power is normalized so that the plane $p=1$ is the (one-dimensional) free-space power. In (a) we restrict the frequency domain to $Kd\in(0,4)\cong(0,1.27\pi)$ to highlight the passband that runs from $Kd=0$ to $Kd\cong0.42\pi$. In the electronic Kronig-Penney model there is no band at zero frequency [12]. However, in this photonic case a band occurs at $\omega=0$, indicating that a constant electric field or very-long-wavelength waves do not feel the effect of the lattice. We see that at the trailing band edge at $Kd\cong0.42\pi$, edge effects arising from a sharp increase in mode density enhance the power output slightly over the free-space plane $p=1$. This effect is due to the fact that the mode density increases near the band edge and that, from the classical version of Fermi's golden rule, Eq. (1), the radiation rate is proportional to this density. In (b) we extend $Kd\in(0,8)\cong2.55\pi$ to see the effects of the next band beginning at $Kd=2\pi$. Bands begin when $Kd=n\pi$, which are precisely the resonant frequencies or "bands" in the parallel mirror model, Fig. 2, if the mirror spacing and the lattice period are both equal to d. This means that in our photonic band structure, Fig. 3, a band always *begins* when an integral number of half-wavelengths fit between the δ functions. We call band frequencies ω frequencies which are "resonant" with the lattice. However, the bands are not infinitely narrow as in the mirror model, allowing here some leeway in the range of resonant frequencies. The behavior of $p(Kd,x/d)$ as a function of x is very similar to that of the mirror model, Fig. 2, for the bands beginning at $Kd=n\pi$ for $n=1,2,\ldots$. As we can see in both (a) and (b), for the band beginning at $Kd=n\pi$ there is an enhancement and a suppression of the radiation rates tracking the maxima and minima of the square of the normal-mode wave function $a_{\omega/c}(x)$, just as in the mirror model. However, now in addition we see a strong enhancement at the trailing band edge, due to the sharp increase in mode density, Eq. (47), there. So an emission enhancement by a factor of about 30 over the free-space rate is seen to be possible due to this edge effect.

the parallel mirror case, it is easy to see that the power radiated is proportional to the square of the normal-mode wave function, i.e., $p(\alpha,\xi) \propto |a_\alpha(\xi)|^2$. In quantum electrodynamical terms, there are no vacuum fluctuations in the band gaps to stimulate emission, and so none occurs. In the frequency passbands the vacuum fluctuations must be normal-mode solutions of the periodic wave equation. The fluctuations have maximum amplitude at the antinodes and minimum amplitude at the nodes of the normal-mode solution $a_k(x)$. The spontaneous emission rate tracks these minima and maxima, as can be seen in Fig. 5(b).

IV. SUMMARY AND CONCLUSIONS

In Sec. I we derived a general classical theory for radiation rates of a classical source in an inhomogeneous medium, as embodied in Eq. (23). We then specialized this result to an oscillating point dipole for the current source and showed how the emission rate depended upon the boundary conditions through the normal-mode functions $\mathbf{a}_\mathbf{k}(\mathbf{r})$, as seen in Eq. (26). We noticed that Eq. (26) also agrees with a fully quantum electrodynamical calculation of Glauber and Lewenstein [11]. We then used this result to recover the free-space power output of a point dipole as a check. In Sec. II we applied our method to the one-dimensional, scalar problem of the radiation rate of a point dipole between a pair of one-dimensional mirrors of separation d, Eq. (36), and then to a dipole inside a periodic lattice of δ function increases of period d in the dielectric constant. Photonic band structure is studied in the latter case as it affects the radiation rate, Eq. (48), and then compared to a similar result derived for the parallel mirror case. In particular, we have emission quenching in the band gaps, and enhancement and suppression of the radiation rate in the bands as a function of the dipole frequency and the location of the dipole in the lattice. Sharp enhancements of the power output over the free-space value are seen for dipole frequencies near the band edges.

Reference to the wave number $\mathbf{k}$ in our final result for the power output of a localized source, Eq. (26), appears not directly, but rather implicitly, as a subscript for the normal-mode function $\mathbf{a}_\mathbf{k}(\mathbf{r})$ and the modal frequency $\omega_\mathbf{k}$. Hence, in the final analysis it is not $\mathbf{k}$ itself that needs to be determined but rather these two $\mathbf{k}$-dependent properties of the normal-mode structure of the medium. We explicitly state that these two quantities are found as a result of solving the Helmholtz eigenvalue equation, Eq. (8). In a general inhomogeneous medium the solution to this eigenvalue problem will be perhaps analytically intractable, but nevertheless it can always be solved in principle, and in practice it can be solved using a powerful enough computer using computational methods currently developed to study the band structure in different dielectric crystals [10]. The results of such a calculation can then be directly inserted into the formula for the power output of a localized source, Eq. (26). Therefore, any direct calculation of the wave vector $\mathbf{k}$ has been effectively circumvented.

We would like to reemphasize that our formulation for determining the effect of an inhomogeneous dielectric medium on atomic radiation rates is a completely general three-dimensional and fully vectorial theory. Once this has been established, one can then ask if there are any simplified analytical models that give a qualitative physical insight into the mechanism for spontaneous emission suppression and enhancement in a photonic band structure. Such a model, an old standby in the context of solid-state theory, is that of Kronig and Penney. In addition, there is in fact a three-dimensional scalar Kronig-Penney model Hamiltonian for electromagnetic waves in an isotropic, inhomogeneous dielectric photonic band structure. This model has been promoted by John and Wang [15], and for it our one-dimensional results go over directly into a three-dimensional treatment. More realistic models cannot be solved analytically due to the intractable nature of the eigenvalue equation. In such situations numerical treatments of atomic emission rates are called for that are beyond the scope of this paper, but that we hope will be attempted by those who are well equipped with such computer techniques and facilities. Finally, we note that a scalar wave version of our theory is directly applicable to the production of sound in media with an inhomogeneous bulk modulus that exhibits "sonic" band structure [16].

ACKNOWLEDGMENTS

The authors would like to thank A. O. Barut, R. R. Inguva, M. O. Scully, and E. Yablonovitch for interesting discussions that contributed to the development of this work. One of us (J.P.D.) would like to acknowledge the National Research Council for support.

APPENDIX

For those who are queasy about using δ functions directly in the dielectric for a Kronig-Penney model, we show here that the same boundary conditions and dispersion relation in Sec. III can be derived as a limiting case from a periodic array of one-dimensional slabs of nonzero width and of alternating indices of refraction n_1 and n_2, as illustrated in Fig. 6. If we label the three regions I, II, and III in Fig. 6 to be defined as

$$\mathrm{I} \equiv \{x | x \in (b/2, a+b/2)\} , \tag{A1a}$$

$$\mathrm{II} \equiv \{x | x \in (-a/-b/2, -b/2)\} , \tag{A1b}$$

$$\mathrm{III} \equiv \{x | x \in (-b/2, b/2)\} , \tag{A1c}$$

where we have defined $d \equiv a+b$ as the lattice period, the Helmholtz equation in the two types of slabs has one of the two forms:

$$a''(x) + \frac{\omega}{c} n_1 a(x) = 0, \quad x \in (b/2, a+b/2) + nd \tag{A2a}$$

$$a''(x) + \frac{\omega}{c} n_2 a(x) = 0, \quad x \in (-b/2, b/2) + nd \tag{A2b}$$

where $n = 0, \pm 1, \pm 2, \ldots$. Without loss of generality, we may choose solutions of Eq. (A1) in regions I and III as

$$a_\mathrm{I}(x) = Ae^{i\mu x} + Be^{-i\mu x} , \tag{A3a}$$

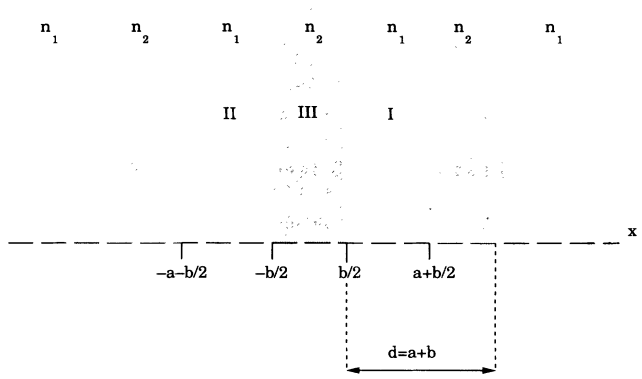

FIG. 6. In the Appendix we derive our δ-function model indicated in Fig. 1 from a nonsingular, one-dimensional model of periodically alternating slabs of indices of refraction n_1 and n_2. We see in this figure that regions I and II are the same as regions I and II in the δ-function model in the limit that the slabs of width b of index n_2, as in region III, vanish as $b\to 0+$. We match the **E** and **B** fields, or, equivalently, $a_k(x)$ and $a_k'(x)$ for continuity at $x=\pm b/2$ and then take the limits $b\to 0$, $a\to d$, $n_1\to 1$, $n_2\to\infty$, $bn_2\to 0$, and $bn_2^2\to gd$, where g is a unitless strength constant for the δ functions, and obtain the same boundary conditions and dispersion relation found in the δ-function model. Hence, the δ-function model used in Sec. III follows cogently in this limit from the more physical model of alternating slabs shown here.

$$a_{\rm III}(x)=Ce^{ivx}+De^{-ivx}\ , \tag{A3b}$$

where we have defined $\mu\equiv\omega n_1/c\equiv Kn_1$ and $\nu\equiv\omega n_2/c\equiv Kn_2$. From Bloch's theorem [12], the form of $a_{\rm II}(x)$ in region II can be generated from $a_{\rm I}(x)$ in region I by

$$\begin{aligned}a_{\rm II}(x)&=e^{-ikd}a_{\rm I}(x+d)\\&=e^{-kd}(Ae^{i\mu(n+d)}+Be^{-i\mu(n+d)})\ ,\end{aligned} \tag{A3c}$$

where k is the wave number of the overall solution $a_k(x)$. Now, the boundary conditions at the slab interfaces, still supposing a magnetic permeability of $\mu=1$, are that the tangential components of **E** and **B** are continuous. (In our one-dimensional model the normal components are zero.) Since $\mathbf{E}=-\partial\mathbf{A}/\partial t$ and $\mathbf{B}=\nabla\times\mathbf{A}$, the two boundary conditions on **E** and **B** can be reexpressed as the demand that the normal modes $a_k(x)$ and their derivatives $a_k'(x)$ are continuous across the interfaces. Hence,

$$a_{\rm I}(b/2)-a_{\rm III}(b/2)=0, \tag{A4a}$$

$$a_{\rm III}(-b/2)-a_{\rm II}(-b/2)=0\ , \tag{A4b}$$

$$a_{\rm I}'(b/2)-a_{\rm III}'(b/2)=0\ , \tag{A4c}$$

$$a_{\rm III}'(-b/2)-a_{\rm II}'(-b/2)=0\ . \tag{A4d}$$

Inserting the normal-mode solutions (A3) into these boundary conditions (A4) yields a 4×4 matrix equation for the four coefficients A, B, C, and D. This system has a nontrivial solution if and only if the transformation matrix has identically zero determinant. This condition leads to the dispersion relation

$$\begin{aligned}\cos(kd)&=\cos(Kn_1a)\cos(Kn_2b)\\&\quad-\frac{n_1^2+n_2^2}{2n_1n_2}\sin(Kn_1a)\sin(Kn_2b)\\&=\frac{(n_1+n_2)^2}{4n_1n_2}\cos[K(an_1+bn_2)]\\&\quad-\frac{(n_1-n_2)^2}{4n_1n_2}\cos[K(an_1-bn_2)]\ ,\end{aligned} \tag{A5}$$

which is that found in the three-dimensional, scalar Kronig-Penney model of a photonic band material employed by John and Wang [15]. In order to take this model over into the limiting case of our periodic array of δ functions, we consider the following limiting case:

$$\begin{aligned}&b\to 0+,\quad bn_2^2\to gd=\text{const}\\&a=d-b\to d,\quad n_2\to\infty\\&bn_2\to 0+,\quad n_1\to 1\ .\end{aligned}$$

We shall now show that this limit recovers the δ-function dielectric model used in Sec. III. The dispersion relation (A5) in the above limit becomes

$$\cos(kd)=\cos(Kd)-\tfrac{1}{2}gKd\sin(Kd)\ , \tag{A6}$$

which is the same as the dispersion relation (44) derived previously for our δ-function lattice. To clinch our argument, we now need to show that the boundary conditions (A4) reduce to the δ-function boundary conditions (39) under the above limits. To this end, we consider the limits

$$\lim_{b\to 0+}[a_{\rm III}(b/2)-a_{\rm III}(-b/2)]=0 \tag{A7a}$$

and

$$\lim_{\substack{b\to 0+\\ bn_2^2\to gd}}[a_{\rm III}'(b/2)-a_{\rm III}'(b/2)]=-gdK^2(C+D)\ , \tag{A7b}$$

where C and D are the wave-function coefficients for $a_{\rm III}(x)$ given in Eq. (A3b). The first condition (A7a) implies that

$$a_{\rm III}(0^+)-a_{\rm III}(0^-)\equiv a_{\rm III}(0)=C+D\ , \tag{A8a}$$

and the second condition (A7b) then gives

$$a_{\rm III}'(0^+)-a_{\rm III}'(0^-)+gdK^2a_{\rm III}(0)=0\ . \tag{A8b}$$

If we now take the limit $b\to 0+$, $bn_2^2\to gd$, etc., in the four boundary conditions (A4) and then use the just-derived singularity conditions (A8) on $a_{\rm III}(0)$ and $a_{\rm III}'(0^{\pm})$ to eliminate these same quantities from the equations, we obtain (upon invoking periodicity) precisely the previously used δ-function condition, Eq. (39). Hence, we have shown that our δ-function model of Sec. III follows in a cogent manner as a limiting case of the more physical model of periodically alternating dielectric slabs.

[1] E. M. Purcell, Phys. Rev. **69**, 681 (1946).
[2] G. Barton, Proc. R. Soc. London, Ser. A **320**, 251 (1970); P. W. Milonni and P. L. Knight, Opt. Commun. **9**, 119 (1973); G. S. Agarwal, Phys. Rev. A **12**, 1475 (1975); A. O. Barut and J. P. Dowling, *ibid.* **36**, 649 (1987).
[3] P. Goy, *et al.*, Phys. Rev. Lett. **50**, 1903 (1983); R. G. Hulet, E. S. Hilfer, and D. Kleppner, *ibid.* **55**, 2137 (1985); G. Gabrielse and H. Dehmelt, *ibid.* **55**, 67 (1985); P. Dobiasch and H. Walther, Ann. Phys. (Paris) **10**, 825 (1985).
[4] S. John, Phys. Rev. Lett. **63**, 2169 (1984); **58**, 2486 (1987).
[5] E. Yablonovitch, Phys. Rev. Lett. **58**, 2059 (1987); E. Yablonovitch and T. J. Gmitter, *ibid.* **63**, 1950 (1989).
[6] G. Kuriziki and A. Z. Genack, Phys. Rev. Lett. **61**, 2269 (1988); G. Kurizki, Phys. Rev. A **42**, 2915 (1990).
[7] H. Morawitz, Phys. Rev. **187**, 1792 (1969).
[8] H. Chew, Phys. Rev. A **38**, 3410 (1988).
[9] J. P. Dowling, M. O. Scully, and F. De Martini, Opt. Commun. **82**, 415 (1991).
[10] E. Yablonovitch, T. J. Gmitter, and K. M. Leung (unpublished); K. M. Leung and Y. F. Liu, Phys. Rev. Lett. **65**, 2646 (1990); Z. Zhang and S. Satpathy, *ibid.* **65**, 2650 (1990); J. W. Haus, H. S. Sözüer, and R. Inguva (unpublished).
[11] R. J. Glauber and M. Lowenstein, Phys. Rev. A **43**, 467 (1991).
[12] D. ter Haar, *Selected Problems in Quantum Mechanics* (Infosearch Ltd., London, 1964), pp. 103–106.
[13] G. Barton, *Elements of Green's Functions and Propagation* (Clarendon, Oxford, 1989), Chap. 10.
[14] J. D. Jackson, *Classical Electrodynamics,* 2nd ed. (Wiley, New York, 1975), Chap. 6.
[15] S. John and J. Wang, Phys. Rev. B **43**, 12 772 (1991).
[16] J. P. Dowling, J. Acoust. Soc. Am. **91**, 2539 (1992).

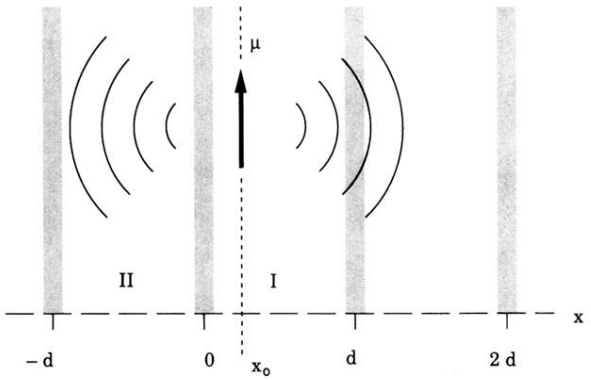

FIG. 3. Here we show a one-dimensional Kronig-Penney model for a photonic band structure that consists of an array of δ-function increases in the dielectric constant $\epsilon(x)$, Eq. (37). We locate a point dipole of frequency ω_0 at a position $x_0 \in (0,d) \equiv \mathrm{I}$ in the first period of the lattice. (From periodicity, the radiation rate in other periods will be the same.) The normal-mode wave functions $a_k(x)$, Eq. (41a), in the lattice period region I are derived by applying Blochs' theorem and appropriate boundary conditions at the δ functions, in particular between regions I and II.

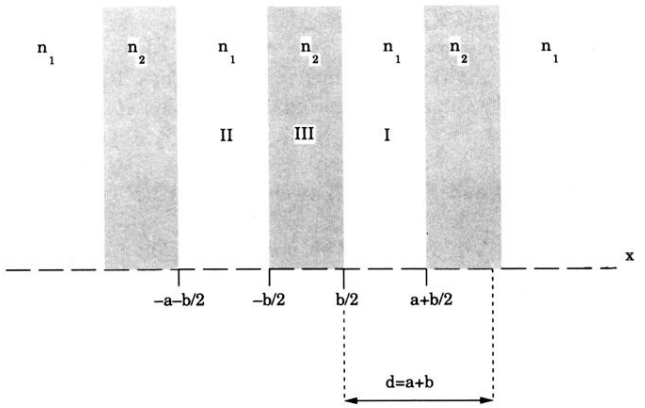

FIG. 6. In the Appendix we derive our δ-function model indicated in Fig. 1 from a nonsingular, one-dimensional model of periodically alternating slabs of indices of refraction n_1 and n_2. We see in this figure that regions I and II are the same as regions I and II in the δ-function model in the limit that the slabs of width b of index n_2, as in region III, vanish as $b \to 0+$. We match the **E** and **B** fields, or, equivalently, $a_k(x)$ and $a_k'(x)$ for continuity at $x = \pm b/2$ and then take the limits $b \to 0$, $a \to d$, $n_1 \to 1$, $n_2 \to \infty$, $bn_2 \to 0$, and $bn_2^2 \to gd$, where g is a unitless strength constant for the δ functions, and obtain the same boundary conditions and dispersion relation found in the δ-function model. Hence, the δ-function model used in Sec. III follows cogently in this limit from the more physical model of alternating slabs shown here.